Supporting Information

Stacey et al. 10.1073/pnas.1211844110

SI Materials and Methods

Diurnal Pattern of Home Cage Ethanol Drinking. The home cage drinking behavior was monitored by a so-called drinkometer e-motion system. This device (INFRA-E-MOTION GmbH) allowed us to study microdrinking patterns and thus, record even very small drinking bouts in the microliter range.

Taste Preference Tests. In alcohol-naïve and -experienced WT and *ras-specific guanine-nucleotide releasing factor 2* (*Rasgrf2*$^{-/-}$) mice, intake of saccharin (sweet) and quinine (bitter) solutions was measured (against water) in a two-bottle free choice test over 9 d. Bottles were weighed, and their positions were changed every 3 d.

Determination of Blood Alcohol Levels. Alcohol-naïve and -experienced WT and *Rasgrf2*$^{-/-}$ mice were injected i.p. with 3.5 g/kg ethanol. Blood alcohol levels were measured by the NADH enzyme spectrophotometric method (Greiner) from blood samples (25–30 μL) drawn from the saphenous vein at 30, 60, 120, and 240 min after injection.

Immunocytochemistry. After a 3-d habituation to handling and injection, mice were injected with ethanol (1 g/kg i.p.) or vehicle (NaCl 9 g/L) (1); 10 min after treatment, mice were anesthetized with pentobarbital (30 mg/kg i.p.; Sanofi-Aventis) and transcardially perfused with 4% paraformaldehyde in phosphate buffer, and brains were taken, postfixed overnight, and cut with a vibratome (Leica) into 30-μm sections stored at −20 °C. Immunohistochemistry was carried out as described (2) using rabbit polyclonal antibodies for active diphospho-ERK (1:500; Cell Signaling Technology), biotinylated anti-IgG antibody (1:500; Vector Laboratories), and avidin–biotin complex (1:500; Vector Laboratories). Bright field microphotographs were analyzed with ImageJ software.

Electrophysiology. ***Electrophysiology.*** Animals (20–40 d) were anesthetized with ketamine (90 mg/kg) /xylazine (15 mg/kg) (Sigma-Aldrich) before preparation of horizontal brain slices (250 μm) containing the ventral tegmental area (VTA). Slicing procedure was done in bubbled ice-cold slicing solution [slicing solution contained choline chloride (110 mM), glucose (25 mM), sodium bicarbonate (25 mM), magnesium chloride (7 mM), ascorbic acid (11.6 mM), sodium pyruvate (3.1 mM), potassium chloride (2.5 mM), sodium dihydrogen phosphate (1.25 mM), and calcium chloride (0.5 mM); artificial cerebrospinal fluid (ACSF) contained sodium chloride (124 mM), sodium bicarbonate (26.2 mM), glucose (11 mM), potassium chloride (2.5 mM), calcium chloride (1.3 mM), magnesium chloride (1 mM), and sodium dihydrogen phosphate (1 mM)]. Brain slices were left to recover in ACSF bubbled with 95% O_2 and 5% CO_2 for 1 h before being transferred to the recording chamber superfused at the rate of 2.5 mL/min. Recordings were made under an Olympus BX51WL. For all recordings, currents were amplified, filtered at 5 kHz, and digitized at 20 kHz. Access resistance was monitored by a hyperpolarizing step of 15-pA injection in current-clamp mode or 10-mV step in voltage-clamp mode [internal solution for voltage-clamp experiments contained caesium chloride (CsCl; 130 mM), NaCl (4 mM), $MgCl_2$ (2 mM), EGTA (1.1 mM), Hepes (5 mM), Na_2ATP (2 mM), sodium creatine phosphate (5 mM), Na_3GTP (0.6 mM), and spermine (0.1 mM)]. Synaptic currents were evoked by stimuli (0.05–0.1 ms) at 0.1 Hz through bipolar glass electrodes filled with ACSF placed rostrally to VTA. The AMPA receptor to NMDA receptor ratio was calculated by dividing the peak amplitudes at +40 mV after digital subtraction of the AMPA + NMDA component and the AMPA component after APV (100 μM). For current-clamp recordings [internal solution contained K-gluconate (140 mM), KCl (5 mM), Hepes (10 mM), EGTA (0.2 mM), $MgCl_2$ (2 mM), Na_2ATP (4 mM), Na_3GTP (0.3 mM), and creatine phosphate (10 mM)], a series of current steps (negative to positive) were injected to induce action potentials. For I_A current, the ACSF was supplemented with 1 μM tetrodotoxin, 0.4 mM cadmium chloride (CdCl2), and 5 mM tetraethylammonium to block Na^+, Ca^{2+} channels and delayed rectified potassium channels. I_A currents were obtained by a two-step protocol, including a first depolarization from −30 to +30 mV and a second depolarization from −120 to +30 mV. The first protocol activates all residual K^+ channels but not I_A, whereas the second protocol activates all K^+ channels including I_A, which was obtained by software-based subtraction of the two components. All recordings were performed at 31–32 °C. Data were collected by a Multiclamp 700B (Molecular Devices) and analyzed by IGOR Wavemetrics (Wavemetrics). Slices were incubated with MEK inhibitors for 1 h before recordings. Dopamine neurons in the VTA were identified by the presence of I*h*.

Genotyping. DNA was extracted from whole-blood samples (~10 mL) preserved in BD Vacutainer EDTA tubes (Becton, Dickinson and Company) using the Gentra Puregene Blood Kit (QIAGEN) according to the manufacturer's instructions. Genotype information was collected at 582,982 markers using the Illumina HumanHap610 Genotyping BeadChip (Illumina). SNPs with call rates of <98%, minor allele frequency <1%, or deviation from the Hardy–Weinberg equilibrium ($P \leq 1 \times 10^{-4}$) were excluded from the analyses. Individuals with an ambiguous sex code, excessive missing genotypes (failure rate > 2%), and outlying heterozygosity (heterozygosity rate of 3 SDs from the mean) were also excluded. Identity-by-state similarity was used to estimate cryptic relatedness for each pair of individuals using PLINK software. Closely related individuals with identity by descent > 0.1875 were eliminated from the subsequent analysis. Population stratification for the genotyping data was examined by principle component analysis using EIGENSTRAT software. The four HapMap populations were used as reference groups in the principle component analysis, and individuals with divergent ancestry (from Central European origin) were also excluded.

Neuroimaging Analyses. ***Monetary incentive delay task.*** This version of the monetary incentive delay task consisted of 66 10-s trials. In each trial, participants were presented with one of three cue shapes (cue = 250 ms) denoting whether a target (white square) would subsequently appear on the left or right side of the screen and whether 0, 2, or 10 points could be won in that particular trial. After a variable delay (4,000–4,500 ms) of fixation on a white cross-hair, participants were instructed to respond with a left or right button press as soon as the target appeared. Feedback on whether and how many points were won during the trial was presented for 1,450 ms after the response. A tracking algorithm adjusted task difficulty (i.e., target duration varied between 100 and 300 ms), and therefore, each participant successfully responded on ~66% of trials. For each 5 points won, the participant would receive one food snack in the form of small chocolate candies. Only successfully hit trials were included for analysis.

Functional MRI data analysis. Functional MRI data were analyzed with SPM8 (Statistical Parametric Mapping; http://www.fil.ion.ucl.ac.uk/spm). Slice-time correction was conducted to adjust for time differences caused by multislice imaging acquisition, all

volumes were aligned to the first volume, and nonlinear warping was performed to an echo planar imaging (EPI) template. Images were then smoothed with a Gaussian kernel of 5-mm full width at half-maximum. At the first level of analysis, changes in the BOLD response for each subject were assessed by linear combinations at the individual subject level for each experimental condition, and each trial (i.e., reward anticipation high gain; reward feedback high gain) was convolved with the hemodynamic response function to form regressors that account for potential noise variance associated with the processing of reward anticipation. Estimated movement parameters were added to the design matrix in the form of 18 additional columns (3 translation, 3 rotation, 3 quadratic, and 3 cubic translation columns, and each 3 translations had a shift of ±1 repetition time). Single-subject contrast images were normalized to Montreal Neurological Institute space. The normalized and smoothed single-subject contrast images were then taken to a second-level random effects analysis. Using the Marsbar toolbox (http://marsbar.sourceforge.net), the VS region of interest was extracted from the anticipation high gain vs. baseline contrast as well as the feedback high gain vs. baseline contrast. The extracted region of interest was based on the work by O'Doherty et al. (3) ($x, y, z = \pm$ 15, 9, −9; radius of 9 mm).

Bioinformatic Analyses. The SNP prioritization tool within pupasuite 3 (http://pupasuite.bioinfo.cipf.es/) was used to obtain putative functional annotation data pertaining to human SNPs (i.e., coding or noncoding; is there overlap with evolutionary conserved chromosomal regions or transcription factor binding sites?). The spatiotemporal mRNA expression of *RASGRF2* in humans was investigated using data from the BrainSpan Atlas of the Developing Human Brain (http://www.brainspan.org/) and the Allen Brain Atlas (http://www.brain-map.org/).

Human Brain Tissue and Genotype-Specific Expression. Brains from male control individuals ($n = 42$) were obtained at autopsy at the Department of Forensic Medicine, Semmelweis University Medical School (Budapest). Causes of death in control subjects were acute cardiac failure or traffic accident. Control participants did not have psychiatric illness or alcohol or drug abuse during the last 10 y. The brains were microdissected and stored in the Human Brain Tissue Bank, Budapest. After removal from the skull, the brains were rapidly frozen on dry ice and stored at −70 °C until microdissection (2 d to 2 mo later). At time of dissection, the brain samples were sliced into 1- to 1.5-mm coronal sections at 0–10 °C. The dorsomedial prefrontal cortex (Brodmann area 9) was dissected just dorsal to the frontopolar area, including the most anterior portions of the superior and middle frontal gyri. The samples were stored at −80 °C until further use. Tissue harvesting occurred after written informed consent was obtained from next of kin and local ethics committee (Semmelweis University) approval. Sample preparation and gene expression assay were as described (4, 5). The following primers were used for quantitative RT-PCR: *RASGRF2* forward: 5′-GCTTGTATACCTCTCTCTCCTGGT-3′ and *RASGRF2* reverse: 5′-ACGCCCATTTTCCAGGTA-3′; *GAPDH* (housekeeping gene) forward: 5′-CATGAGAAGTATGACAACAGCCT-3′ and *GAPDH* reverse: 5′-AGTCCTTCCACGATACCAAAGT-3′. The relative gene expression levels of *RASGRF2* to *GAPDH* (ΔCt) were transformed using normal quantile transformation. We used a generalized linear model to assess the effect of allele on *RASGRF2* mRNA levels, with sex, age, postmortem interval, and RNA integrity number included as covariates.

IMAGEN Consortium. IMAGEN Consortium: Albrecht, L., Andrew, C., Arroyo, M., Artiges, E., Aydin, S., Bach, C., Barbot, A., Boddaert, N., Bokde, A., Bricaud, Z., Bromberg, U., Bruehl, R., Cachia, A., Cattrell, A., Constant, P., Crombag, H., Czech, K., Dalley, J., Decideur, B., Fadai, T., Fernandes, A., Frouin, V., Fuchs, B., Gollier Briand, F., Gowland, P., Head, K., Heinrichs, B., Heym, N., Hübner, T., Ihlenfeld, A., Ireland, J., Ivanov, N., Jones, J., Kepa, A., Klaassen, A., Lalanne, C., Lanzerath, D., Lemaitre, H., Lubbe, S., Lüdemann, K., Mallik, C., Mangin, J.-F., Mar, A., Martinez-Medina, L., Massicotte, J., Mennigen, E., Mignon, X., Miranda, R., Müller, K., Paillere, M.-L., Pena-Oliver, Y., Poline, J.-B., Poustka, L., Rapp, M., Reed, L., Reuter, J., Ripke, S., Ripley, T., Robbins, T., Rodehacke, S., Rogers, J., Romanowski, A., Schilling, C., Schmäl, C., Schmidt, D., Schneider, S., Schroeder, M., Schubert, F., Schwartz, Y., Speiser, C., Spranger, T., Steiner, S., Stephens, D., Strache, N., Ströhle, A., Struve, M., Subramaniam, N., Tahmasebi, A., Theobald, D., Topper, L., Vollstaedt-Klein, S., Walaszek, B., Werts, H., Whelan, R., Williams, S., Yacubian, J., Ziesch, V., Zibovicius, M., and Wong, C. P.

1. Bertran-Gonzalez J, et al. (2008) Opposing patterns of signaling activation in dopamine D1 and D2 receptor-expressing striatal neurons in response to cocaine and haloperidol. *J Neurosci* 28(22):5671–5685.
2. Valjent E, Pagès C, Hervé D, Girault J-A, Caboche J (2004) Addictive and non-addictive drugs induce distinct and specific patterns of ERK activation in mouse brain. *Eur J Neurosci* 19(7):1826–1836.
3. O'Doherty J, et al. (2004) Dissociable roles of ventral and dorsal striatum in instrumental conditioning. *Science* 304(5669):452–454.
4. Schumann G, et al. (2011) Genome-wide association and genetic functional studies identify autism susceptibility candidate 2 gene (AUTS2) in the regulation of alcohol consumption. *Proc Natl Acad Sci USA* 108(17):7119–7124.
5. Sommer WH, et al. (2010) Human NPY promoter variation rs16147:T>C as a moderator of prefrontal NPY gene expression and negative affect. *Hum Mutat* 31(8): E1594–E1608.

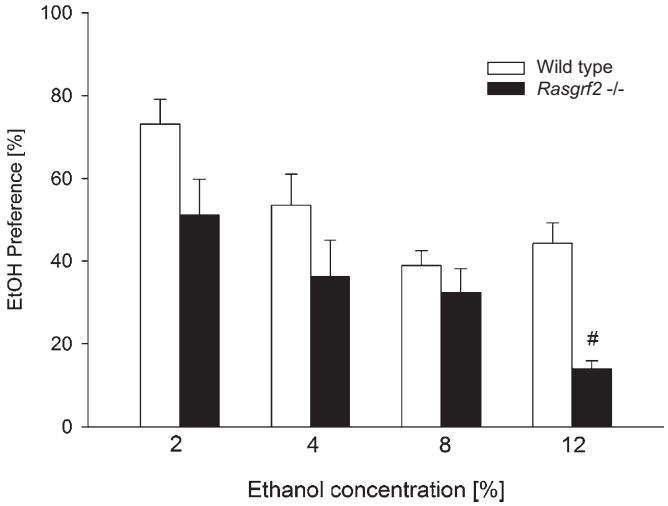

Fig. S1. Ethanol preference (n = 12–13) is reduced in male *Rasgrf2*$^{-/-}$ relative to WT controls. Preference data are expressed as percentage of intake of ethanol-containing solutions relative to water. A two-way ANOVA revealed a significant genotype effect ($F_{1,23}$ = 12.3; $P < 0.01$) and concentration effect ($F_{3,69}$ = 13.5; $P < 0.0001$) but not a significant genotype × concentration interaction effect ($F_{3,6}$ = 1.6; P = 0.2) on ethanol preference. $^{\#}P < 0.05$.

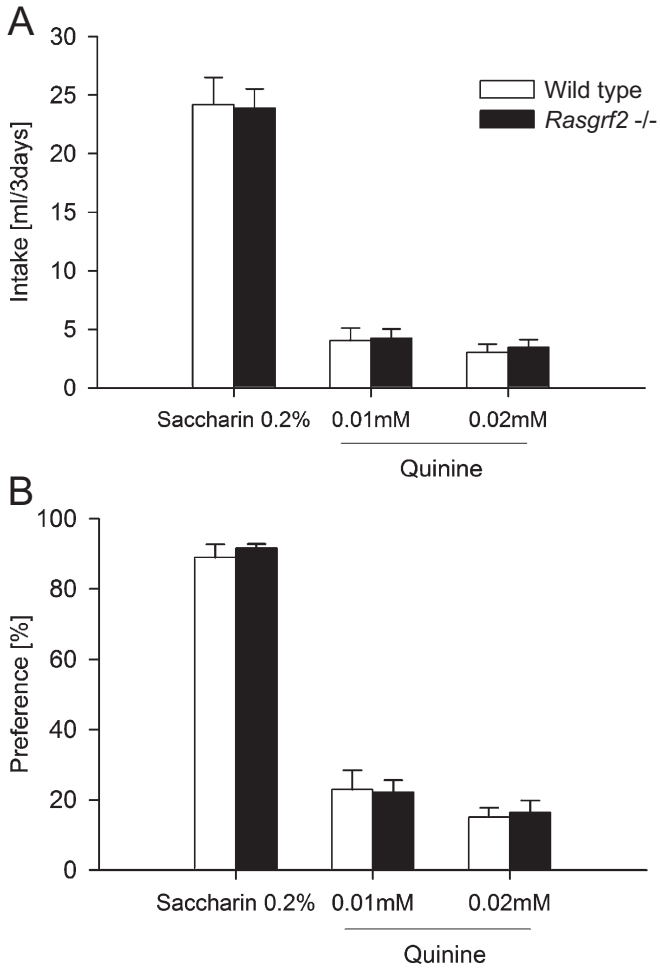

Fig. S2. No difference in taste sensitivity between male *Rasgrf2*$^{-/-}$ mice (n = 8–13 per solution) and WT controls (n = 6–9 per solution). Mean intake (*A*) and preference (*B*) of sweet (saccharin) over bitter (quinine) solutions over a 3-d period. A two-way ANOVA revealed a significant effect of solution (for intake: $F_{2,46}$ = 141.8; $P < 0.0001$; for preference: $F_{2,46}$ = 426.5; $P < 0.0001$) but not of genotype (for intake: $F_{1,46}$ = 0.009; P = 0.9; for preference: $F_{1,46}$ = 0.2; P = 0.7).

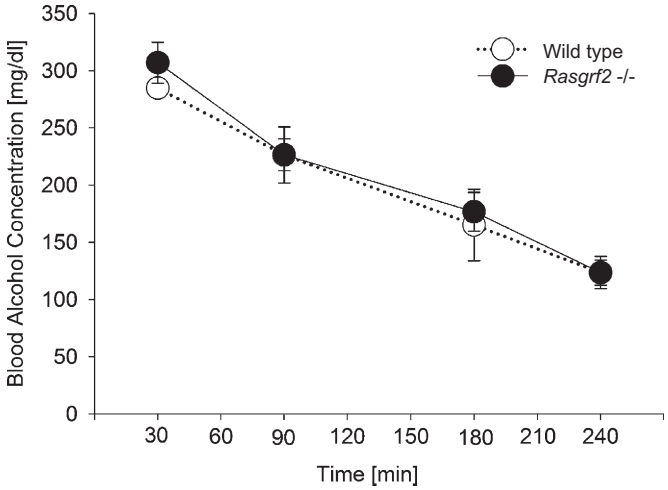

Fig. S3. No difference in blood ethanol elimination between *Rasgrf2*$^{-/-}$ mice (n = 6–8 per time point) and WT controls (n = 6–7 per time point). Blood ethanol elimination measurements taken at 30, 90, 180, and 240 min after an i.p. injection of 3.5 g/kg ethanol. A two-way ANOVA revealed a significant effect of time ($F_{3,47}$ = 37.8; P < 0.000001) but not genotype ($F_{1,47}$ = 0.4; P = 0.5).

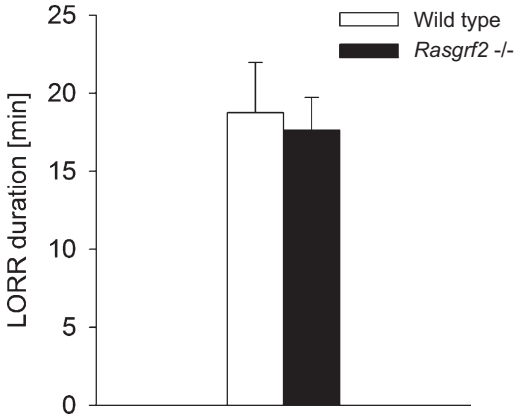

Fig. S4. No difference in duration of loss of righting reflex between *Rasgrf2*$^{-/-}$ mice (n = 11) and WT controls (n = 13). Loss of righting reflex duration after an i.p. injection of 3.5 g/kg ethanol (t_{22} = 0.3, P = 0.8).

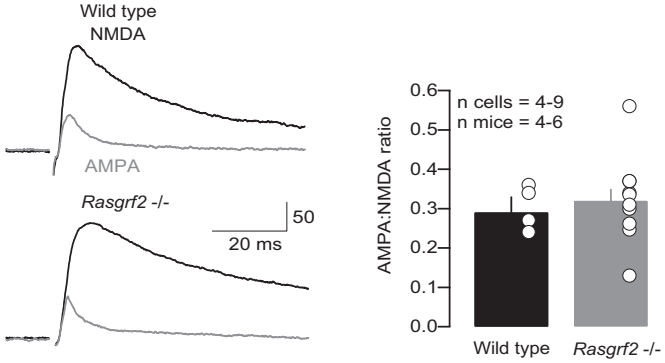

Fig. S5. No difference in synaptic input to the VTA between *Rasgrf2*$^{-/-}$ mice and WT controls. AMPA:NMDA ratios derived from excitatory postsynaptic currents (t_9 = 0.8, P > 0.05).

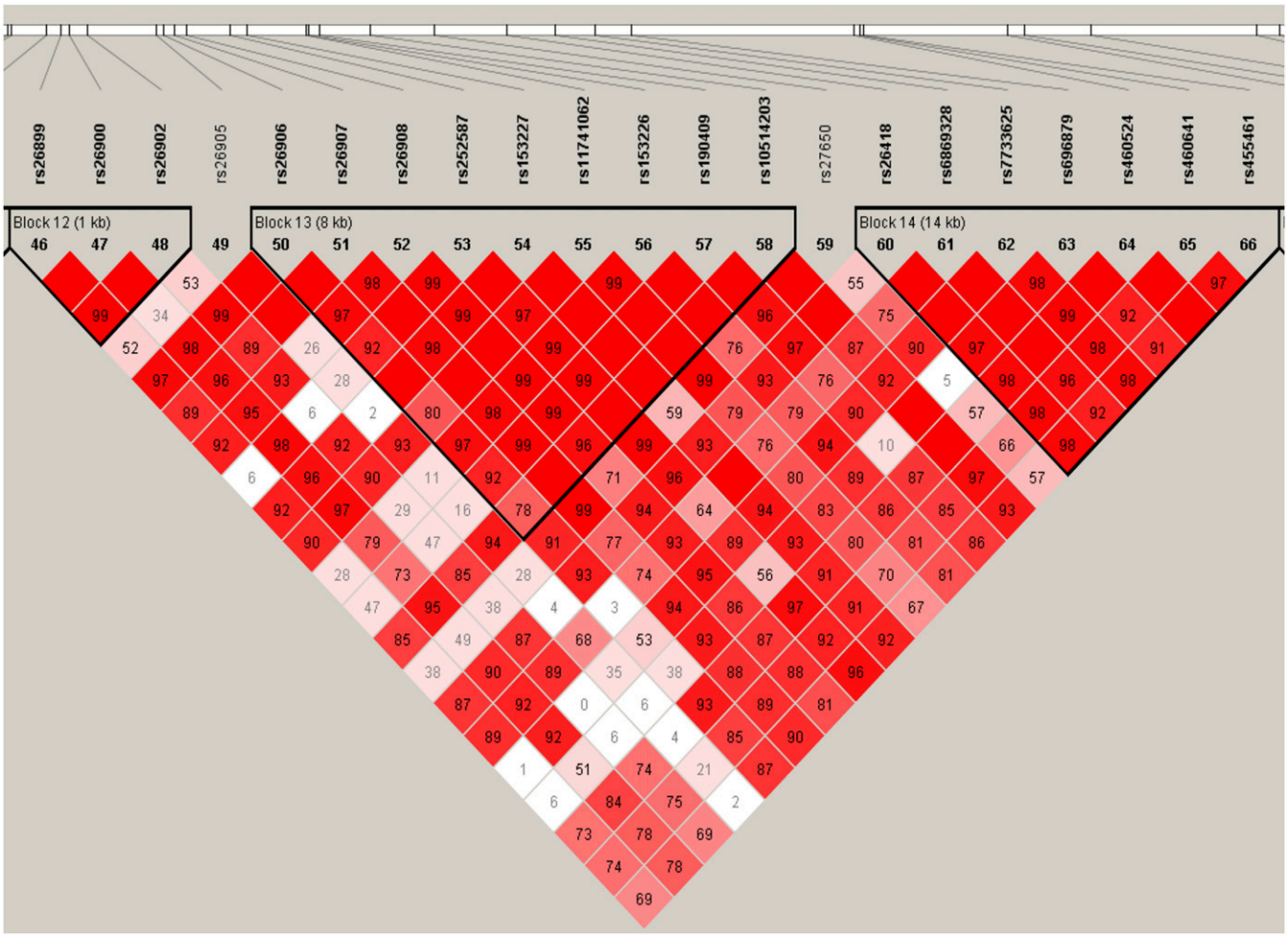

Fig. S6. Linkage disequlibrium (LD) plot for the haplotype block (block 13) containing rs26907. Generated according to Four Gamete Rule with threshold 0.01 from Haploview.

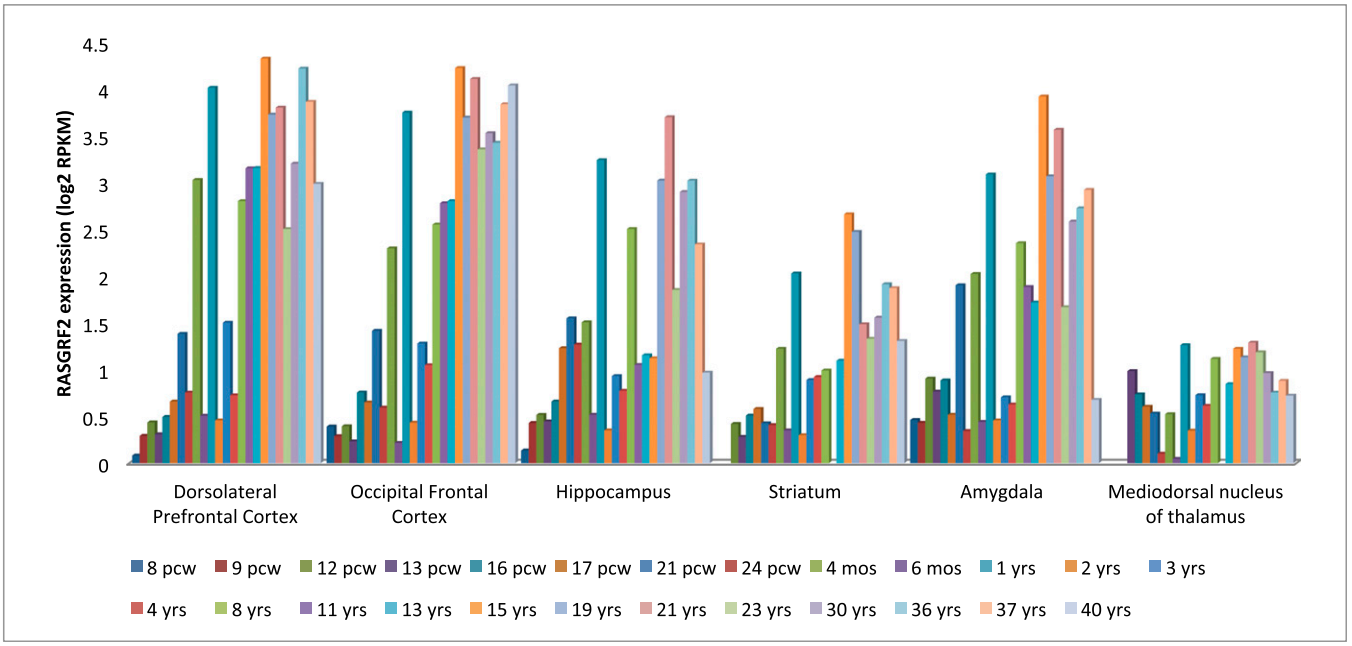

Fig. S7. Spatiotemporal mRNA expression patterns of *RASGRF2* in humans. Data were extracted from Brain Span, Atlas of Developing Human Brain.

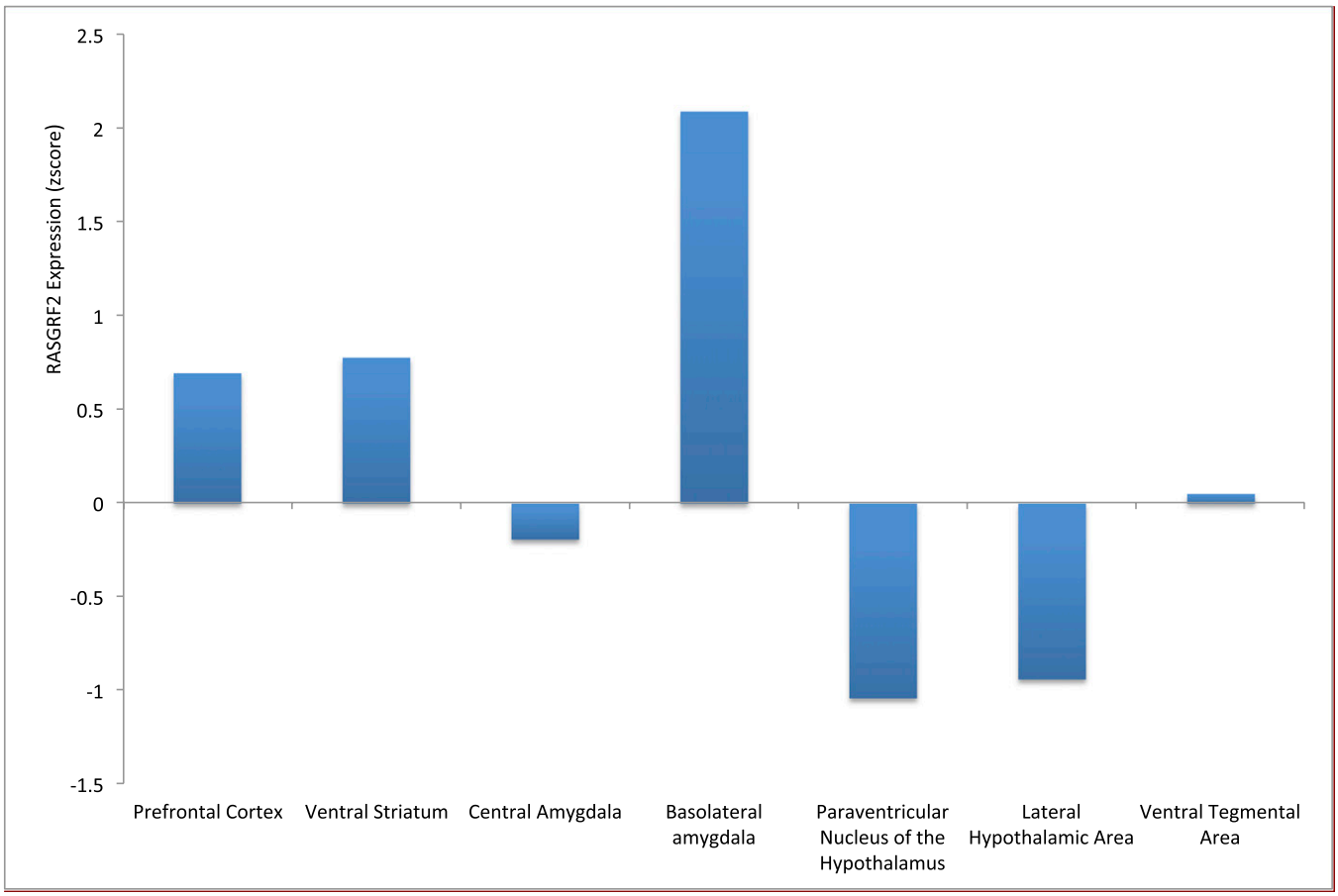

Fig. S8. Regional mRNA expression of human *RASGRF2* in the VTA relative to other brain areas. Data were extracted from the Allen Human Brain Atlas and were generated using Agilent 8 × 60,000 gene expression arrays. Relative *RASGRF2* mRNA levels are expressed as *z* scores.

Table S1. Haplotype phases of haplotype block generated using the Four Gamete Rule with a threshold of 0.01 ordered by their frequencies

	rs26906	rs26907	rs26908	rs252587	rs153227	rs11741062	rs153226	rs190409	rs10514203	Frequency
Hap1	C	G	T	A	A	A	T	A	G	0.2443
Hap2	C	G	T	G	A	C	T	G	G	0.1584
Hap3	C	A	C	G	G	A	C	G	G	0.1537
Hap4	C	G	T	G	A	A	T	A	G	0.1143
Hap5	C	G	C	G	A	A	C	G	G	0.09121
Hap6	C	G	C	G	G	A	C	G	G	0.08522
Hap7	T	G	T	A	A	A	T	A	G	0.07633
Hap8	C	G	T	G	A	A	C	G	A	0.06225

Other Supporting Information Files

SI Appendix (DOC)